PRAMANA — journal of physics

Vol. 80, No. 5
May 2013
pp. 873–885

The measurements of thermal neutron flux distribution in a paraffin phantom

PARISA AKHLAGHI*, LALEH RAFAT-MOTAVALLI and SEYED HASHEM MIRI-HAKIMABAD

Physics Department, Faculty of Sciences, Ferdowsi University of Mashhad, Azadi Square 91775-1436, Mashhad, Iran
*Corresponding author. E-mail: parissa_akhlaghi@yahoo.com

MS received 15 July 2012; revised 16 November 2012; accepted 6 December 2012

Abstract. The term 'thermal flux' implies a Maxwellian distribution of velocity and energy corresponding to the most probable velocity of 2200 m s^{-1} at 293.4 K. In order to measure the thermal neutron flux density, the foil activation method was used. Thermal neutron flux determination in paraffin phantom by counting the emitted rays of indium foils with two different detectors (Geiger–Muller counter and NaI(Tl)) was the aim of this project. The relative differences of the outcome of the experiments were between 2.5% and 5%. The final results were compared with MCNP4C outputs and the best agreement was generated using NaI(Tl) by a minimum discrepancy of about 0.6% for the foil placed 8.5 cm from the neutron source.

Keywords. Thermal neutron flux; foil activation; indium foils; cadmium difference method; Geiger–Muller counter; NaI(Tl).

PACS Nos 29.30.Kv; 23.40.−s; 28.20.Np; 29.40.Cs

1. Introduction

Neutron detection by foil activation is based on the formation of a radioisotope by neutron capture, and subsequent counting of the radiation emitted by that radioisotope. Because neutrons are difficult to detect, neutron activation is used to produce γ-rays and β-particles, which are proportional to the neutron flux and are easier to detect [1].

The most commonly used neutron reaction is the (n, γ) reaction, which takes place with almost all isotopes with different probability and has no threshold. In general, the (n, γ) cross-section is higher for thermal than for fast neutrons. The advantages of γ-rays are well known in terms of low effect by self-shielding and backscattering in the foil.

Foil is extremely thin, usually metallic and has many advantages over other types of detectors: it is (1) relatively cheap, (2) small in size, (3) insensitive to γ-rays and (4) easy to handle. By virtue of its small thickness, flux determination by using a foil results

DOI: 10.1007/s12043-013-0524-5; ***e*Publication: 12 April 2013**

in minimum perturbation of the neutron flux and a minimum of self-shielding. A thick sample will absorb so many neutrons that the radiation field will be perturbed and this perturbation causes flux depression in its interior [2].

Four indium foils were placed in front of the neutron source in a paraffin phantom. The emitted γ- and β-rays were collected by Geiger–Muller counter and NaI(Tl) and then, thermal flux was determined at the foils' position.

2. Methods

The division of neutron spectrum in two energy groups is possible through the resonance absorption property of cadmium. The absorption cross-section of cadmium is large at low energies, but as the energy increases above 0.5 eV the cross-section begins to decrease drastically. It means that cadmium captures almost all thermal neutrons and lets the epithermal ones pass. Thus, by comparing the activity induced in bare foils to that induced in cadmium-covered foils, the activity resulting from neutrons of the two energy groups is calculated [3]. Absolute activities are computed from the measured count rates by applying various correction factors. From these absolute activities, flux values are computed for both thermal and epithermal neutrons. Cadmium difference method requires that the foil detectors be thin so that the self-shielding and neutrons flux perturbation are small. For this purpose, a specimen is placed in front of the neutron source once with a cadmium cover (with 0.5–1.5 mm thickness) and once without cadmium cover. The cadmium cover over the foil during the activation process, prevented thermal energy neutrons from reaching the foil [4–6]. Therefore, in the presence of cadmium only epithermal neutrons activate the specimen [7].

When a thin foil of the target atoms is placed in a neutron flux its activity increases exponentially until the activity reaches a saturation value. If the activity does not reach saturation, the activity, A_0, of the foil after the irradiation time (t_i) is given by

$$A_0 = \lambda N(t) = A_s(1 - e^{-\lambda t_i}), \tag{1}$$

where A_s is the saturation activity and λ is the decay constant. If a foil is irradiated nine times of its half life, with 0.4% error, the activity will be equal to saturation activity.

Before counting and with respect to the half-life of the products, one considers a delay time (t_d) to remove the interfering activities of impurities. If the counting is carried out over an interval between t_d and t_{d+c}, the number of counts measured will be

$$N_0 = \varepsilon \frac{A_0}{\lambda} e^{-\lambda t_d} \left(1 - e^{-\lambda t_c}\right) + B, \tag{2}$$

where ε is the overall counting efficiency, B is the number of background counts expected in t_c and N_0 is the difference between count rates of the foils with and without cadmium cover. The saturation activity is given by

$$A_s = N_T \sigma_{ath} \phi_{th}, \tag{3}$$

where N_T is the total number of target atoms in the detector and σ_{ath} is the thermal absorption cross-section. It is often convenient to replace the total number of target atoms N_T by

$$N_T = \frac{N_A m}{M}. \tag{4}$$

In this equation N_A is the Avogadro's number, m is the mass of the specimen and M is the atomic mass. By combining eqs (1)–(3) and applying the correction factors, thermal neutron flux in units of neutrons $\cdot\text{cm}^{-2}\cdot\text{s}^{-1}$ was obtained [8–10], which can be calculated by

$$\phi_{\text{th}} = \frac{N_0\lambda}{N_T\sigma_{\text{th}}\varepsilon g I G_{\text{th}}(1-\text{e}^{-\lambda t_i})\text{e}^{-\lambda t_d}(1-\text{e}^{-\lambda t_c})}, \tag{5}$$

where G_{th} is the thermal neutron self-shielding factor in foils, I is the intensity of the emitted ray line at observed spectra and g is the Westcott factor which describes the deviation of the cross-section from a $1/v$ shape [11].

2.1 *Correction factors*

The thermal neutron self-shielding factor, G_{th}:

If an absorbing sample is located in neutron field, the interior of the sample will be exposed to a smaller neutron flux than the exterior because of the absorption of neutrons within the foil. In general, the interpretation of the sample activation due to thermal neutrons requires the knowledge of this parameter. The thermal neutron self-shielding is given by

$$G_{\text{th}} = \frac{1}{1+\left(\frac{N_A k_{\text{th}}}{r(r+h)}\sum_j \frac{m_j\sigma_{a,j}}{M_j}\right)}. \tag{6}$$

This equation is used to calculate thermal neutron self-shielding factors in a cylindrical sample irradiated in a nearly isotropic neutron field. N_A is the Avogadro's number, k_{th} is the thermal self-shielding constant, m_j is the amount of element j (g), $\sigma_{a,j}$ is the thermal neutron absorption cross-section, M_j is the atomic mass of the element j, r and h are radius and height of the cylinder, respectively [12–14].

Westcott factor, g:

This factor represents the deviation of the cross-section in the thermal range. If $\sigma(v)$ varies as $1/v$, the Maxwellian cross-section is equivalent to 2200 $\text{m}\cdot\text{s}^{-2}$ and $g = 1$. This factor is given by

$$g(\text{Temp}) = \frac{\int_0^\infty \sigma(v) n_{\text{Temp}}(v) v\,\text{d}v}{\sigma_0 v_0 \int_0^\infty n_{\text{Temp}}(v)\,\text{d}v}, \tag{7}$$

where v is the neutron velocity, $n_{\text{Temp}}(v)$ is the neutron density distribution in temperature *Temp*, $\sigma(v)$ is the neutron cross-section at velocity v, v_0 is the thermal neutron velocity which is equal to 2200 $\text{m}\cdot\text{s}^{-1}$ and σ_0 is the neutron cross-section for v_0 neutrons [15].

Cadmium correction factor, F_{Cd}:

Cadmium absorbs some epithermal neutrons and passes some thermal ones. So we should take into account the attenuation of the epithermal neutrons in the cadmium filter and its contribution in the foil activation due to thermal part of the spectrum. Reduction of cadmium thickness will cause a decrease in epithermal neutron absorption [16].

Counting efficiency, ε:

The overall counting efficiency is influenced by many factors: A geometry factor corrects for the fraction of the radiation that is not subtended by the detector, a counter-window correction that corrects the number of β particles or γ-rays absorbed or scattered by the detector window and the counter intrinsic efficiency. ε is the combination of all of these correction factors. So it can be calculated by simulating the whole set-up and specifying the number of β- or γ-rays reaching the detector.

Emission probability, I_β *and* I_γ:

When a foil is irradiated by neutrons, it is likely to emit β- or γ-rays. Gamma rays are related to daughter nuclei and are emitted after β irradiation. If β-rays are certainly emitted then, $I_\beta = 1$ and I_γ is the number of γ-rays emitted per beta. In the case of detecting gamma, one uses the area under the full-energy peaks that appear in the spectrum and checks the emission probability.

2.2 *Specification of indium foils*

Indium has two naturally occurring isotopes, ^{113}In (4.3%) and ^{115}In (95.7%). ^{113}In is the only stable isotope of indium and has a relatively small thermal cross-section of only 4 barns. It is activated to ^{114}In that has a 72-s half-life. Due to the paucity of ^{113}In in natural indium and its lower cross-section, this activation is only a minor radiator from the activated indium.

^{115}In is activated to three products, ^{116}In, ^{116m1}In and ^{116m2}In. ^{116}In has a half-life of about 13 s and ^{116m2}In has a short half-life (2 s) and a very low cross-section for this reaction. ^{116m1}In is the ultimate activation product. This is due to its long half-life of 54 min and ^{115}In's large cross-section (154 barns) for this particular reaction [17]. Therefore, of the four possible reactions with neutron absorption, our desire is to form ^{116m1}In, which produces three gammas, 417 keV, 1097 keV and 1293 keV, and a 1 MeV beta particle. The decay scheme of ^{116m1}In is shown in figure 1 (the scales are not accurate). In this figure, only important energies of γ-rays are shown [18].

For indium foils, the Westcott factor is 1.019 [19] and decay constant is 0.0128 min^{-1}. Decaying ^{116m1}In, definitely, produces beta and so $I_\beta = 1$ and by summing the number of γ-rays emitted per beta, the obtained $I_\gamma = 2.52$.

The indium foils, which were tested, had a radius of 1.25 cm and a thickness of about 0.112 cm. In this experiment, four indium foils were placed at distances of 6, 8.5, 11 and 13.5 cm from the neutron source. For convenience, we named these foils No. 1, No. 2, No. 3 and No. 4, respectively. Their weights, with respect to the distance from the source, were 2.106, 2.089, 2.126 and 2.11 g. Based on eq. (6), thermal neutron self-shielding factor were 0.5288, 0.5307, 0.5265 and 0.5282, respectively.

2.3 *Neutron source*

For the experimental study, Am–Be was used as a source of thermal and epithermal neutrons. The Am–Be source, at Ferdowsi University of Mashhad, had a 3.94 Ci activity. It

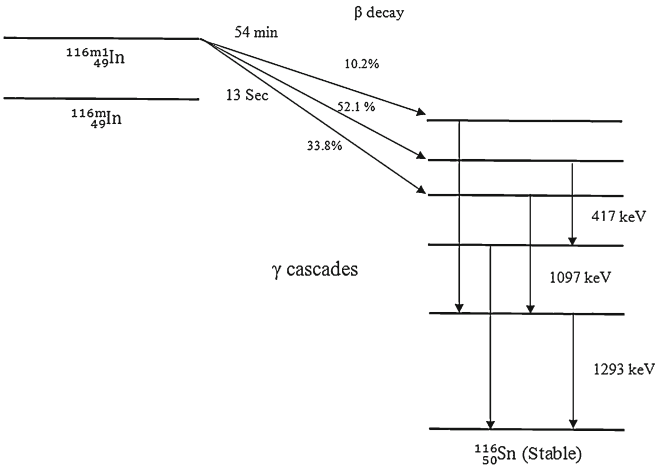

Figure 1. Simplified decay scheme of ^{116m1}In.

sends out almost 2200 neutrons per 1 mCi in 1 s and so the number of neutrons which are generated by the source are 8.65×10^6.

The source was in the form of a homogeneous sphere, which was in a cylinder of paraffin with about 0.94 g·cm^{-3} density. The radius and height of the cylinder were 30 cm and 60 cm, respectively. An air cylinder was embedded in it, along the positive direction of the cylinder axis 2 cm away from the centre of the paraffin cylinder, with 2.5 cm radius and 28 cm height. Am–Be was set on the cylinder axis 16 cm from the bottom of the air cylinder. To bring the foils in or out, there was an aperture perpendicular to the cylinder axis with 2 cm radius and 25 cm height, that the distance between the bottom of the aperture and the centre of paraffin cylinder was about 5 cm. The foils were placed in a cylinder made of Plexiglas with 1 g·cm^{-3} density. A view of the neutron source, Plexiglas cylinder and indium foils is given in figure 2.

2.4 *Determination of thermal neutron flux by Geiger–Muller counter*

To measure the activity resulting from neutron exposure, after the irradiation, the foil was transferred to a detector. Once removed from the neutron flux, the activity of the foil was continually decreasing exponentially. Therefore

$$\ln(N) = \ln(N_0) - \lambda t, \tag{8}$$

where N and N_0 are the number of radioactive nuclei in time t and t_0, respectively.

For counting β- and γ-rays, a Geiger–Muller counter was used. After passing time of about half-life of indium, activity would decrease and thus the statistical errors increase. Therefore, detecting the rays reaching the counter was done in about 30 min, with a delay time and counting time of 5 min and 1 min, respectively. By plotting the diagram $\ln(N_0)$ vs. t we obtained N_0 which is proportional to A_0, the activity at $t = 0$,

$$N_0 = \varepsilon l A_0. \tag{9}$$

Figure 2. A view of paraffin phantom, Plexiglas cylinder, indium foils and aperture. Neutron source is 18 cm above the aperture.

To determine N_0, the emitted rays from the foils with and without cadmium cover were counted. By combining eqs (1), (3), (9) and considering the delayed time, the thermal flux would be

$$\phi_{\text{th}} = \frac{N_0}{N_{\text{T}}\sigma_{\text{th}}\varepsilon g I G_{\text{th}}(1 - \text{e}^{-\lambda t_{\text{i}}})\text{e}^{-\lambda t_{\text{d}}}}, \tag{10}$$

where all the symbols have the same meaning as in eq. (5).

2.5 *The secondary gamma spectroscopy by NaI(Tl)*

$^{116\text{m}1}$In produces three characteristics γ-rays with energies about 417 keV, 1097 keV and 1293 keV. By counting the gamma reaching the detector, one can specify the area under the each photopeak that appears in the spectrum. It should be mentioned that the energy resolution of NaI(Tl) for γ-rays of ^{137}Cs (0.662 MeV) was about 9.5% in our case, which was calculated as the FWHM divided by the location of the peak.

Table 1. Counting results for bare indium foil placed 6 cm from the source.

t (min)	Counts (N')	Net counts (N)	σ_N
5.5	8701	8678.4	93.40021
11.5	8137	8114.4	90.3305
17.5	7429	7406.4	86.32265
23.5	7121	7098.4	84.51982
29.5	6537	6514.4	80.99136

To calibrate the NaI(Tl), two γ emitters, ^{137}Cs and ^{60}Co, were placed in front of the detector. After the irradiation and 5 min delay in enumeration, foils were placed in front of NaI(Tl) and the γ-rays were counted for 2 h. To determine the thermal flux, the counting curve vs. channel was plotted for all the foils with and without cadmium cover.

3. Results and discussion

The four foils were irradiated for 8 h (almost nine half-lives), then they were removed from the source and after 5 min, which are necessary to eliminate ^{116m2}In and ^{113}In, counting was started.

3.1 *Flux determination by Geiger–Muller counter*

The number of background counts for bare indium was 113 and for cadmium-covered foil it was 104. The results of experiments by Geiger–Muller for foil No. 1 are given in table 1. The experiment was repeated for the foils with cadmium cover and the final results of two steps for foil No. 1 are shown in table 2. Such results were attained for the other indium foils. According to eq. (8), for four indium foils $\ln(N)$ vs. time and its linear fit are plotted in figure 3.

In another simulation with MCNP4C, the counting efficiency and cadmium correction factor were specified. To determine the counting efficiency, an indium foil, once as a β source and the other time as a γ one, was placed inside paraffin in the form of a cylinder. The desired tally was F1, which determines the number of γ- or β-rays reaching the

Table 2. The results of two steps for indium foil placed 6 cm from the source.

t (min)	Counting difference in 2 steps	σ_N	$\ln(N)$	$\sigma(\ln(N))$
5.5	7357.675	100.5356	8.903499	0.013664
11.5	6846.811	97.41355	8.831538	0.014228
17.5	6306.091	92.79763	8.749271	0.014716
23.5	6051.227	90.82621	8.708016	0.01501
29.5	5546.931	87.08846	8.621	0.0157

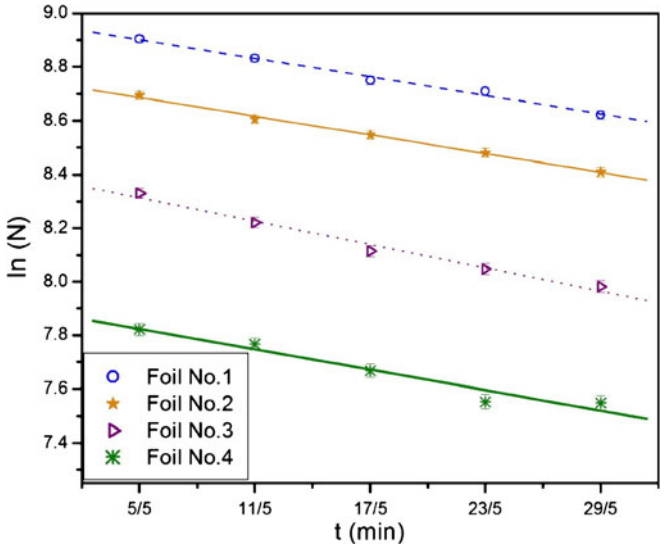

Figure 3. ln(N) vs. time and its linear fit for four indium foils.

counter per one emitted particle. According to Geiger user's manual, its efficiency for counting β- and γ-rays is 100% and 10%, respectively. Combining the Geiger efficiency and program's output, one obtained the counting efficiency, which is about 0.0232 for β- and 0.0486 for γ-rays.

For assigning F_{Cd}, two different programs were run; in the first case epithermal neutrons were radiated to a bare indium foil and in the other one a source of thermal and epithermal neutrons was located in front of a foil with cadmium cover. The desired tally

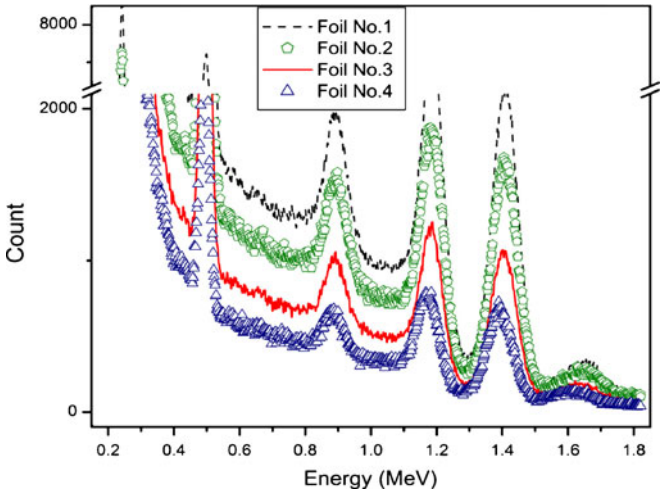

Figure 4. The counting abundance curve vs. energy curve for each of the four foils without cadmium cover.

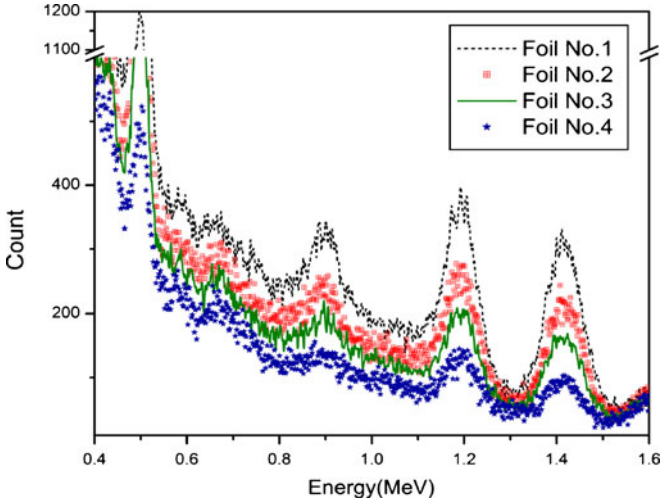

Figure 5. The counting abundance curve vs. energy curve for each of the four foils with cadmium cover.

was F4. Dividing two outputs, the result, for a point source and cadmium thickness of about 0.75 mm, was 0.984.

3.2 *Thermal flux determination using NaI(Tl)*

The abundance curves obtained by NaI(Tl) for bare indium foil and cadmium-covered foil for each of the four foils were shown in figure 4 and figure 5 separately. The area under each peak and the full spectrum of the foils in both cases are given in table 3.

According to the available data, specifying the probability of γ emission for each foil is easy and can be calculated as the sum of the irradiation probabilities of three energies 417 keV, 1097 keV and 1293 keV which is equal to $I_\gamma = 1.685$ [20].

Table 3. The area under the full spectrum for the foils in both cases.

Foil No.	417 (keV)	σ_{417}	1097 (keV)	σ_{1097}	1293 (keV)	σ_{1293}	Total	σ_{T}
1	210041	458.30	149659	386.85	144819	380.55	504519	710.29
1 with Cd	43407	208.34	26279	162.10	23741	154.08	93427	305.65
2	174657	417.91	110595	332.55	112129	334.85	397381	630.38
2 with Cd	32550	180.41	20131	141.88	16073	126.77	68754	262.20
3	116824	341.79	77790	278.90	72254	268.80	266868	516.59
3 with Cd	27103	164.62	14964	122.32	13336	115.48	55403	235.37
4	78027	279.33	49631	222.78	47945	218.96	175603	419.05
4 with Cd	20468	143.06	9760	98.792	7373	85.866	37601	193.90

Table 4. Thermal neutron flux for each foil by experiment and simulation.

Distance from source (cm)	Measured thermal flux ($n \cdot cm^{-2} \cdot s^{-1}$)		
	Geiger	NaI(Tl)	Simulation
6	$1.05 \times 10^3 \pm 40$	$1.10 \times 10^3 \pm 32$	$1.39 \times 10^3 \pm 4.6$
8.5	$8.53 \times 10^2 \pm 32$	$8.86 \times 10^2 \pm 26$	$8.92 \times 10^2 \pm 3.5$
11	$5.95 \times 10^2 \pm 22$	$5.65 \times 10^2 \pm 16$	$5.78 \times 10^2 \pm 2.9$
13.5	$3.60 \times 10^2 \pm 14$	$3.70 \times 10^2 \pm 11$	$3.82 \times 10^2 \pm 2.3$

To calculate ε, MCNP4C simulation was used again. The desired tally was F8 that its output gave the pulse height. The abundance of each peak expressed the number of counted γ in that energy. The gained result for counting efficiency was about 0.0703. By considering the above correction factors and using eq. (5), the thermal neutron flux was calculated for each foil. The results of thermal flux measurements in both steps together with their errors are given in table 4. The data achieved by these two methods were compared with each other and a good agreement was observed. As we can see, their relative differences were between 2.5% and 5%.

Correction factors and their relative errors are summarized in table 5. In addition, changes in flux (in percent) because of the lack of consideration of each of these factors, for two different measuring methods, are expressed. The negative signs are due to the factors, which reduced the amount of flux. By applying these correction factors, the amount of flux measured respectively by NaI(Tl) and Geiger–Muller will be almost 15.73 times and 12.77 times greater than the value without applying any correction.

If the uncertainties consisting of all the correction factors were considered, the maximum relative error in flux estimation with NaI(Tl) and Geiger–Muller counter would be almost about 2.9% and 3.8%, respectively. These total uncertainties were the quadratic sum of both statistical and systematic errors. The contribution of various correction

Table 5. Correction factors, their relative errors and changes in flux (in percent) by not considering each of the factors. ε_β and I_β were defined just for flux determination with Geiger–Muller counter.

Correction factors	G_{th}	g	F_{Cd}	ε_γ (ε_β)	I_γ (I_β)
NaI(Tl)	$0.5285 \pm 1.60\%$	$1.019 \pm 0.10\%$	$0.984 \pm 0.06\%$	$0.0703 \pm 0.08\%$	$1.685 \pm 0.60\%$
Changes in flux in percent	47.15	−1.90	0.37	92.97	−68.50
Geiger–Muller	$0.5285 \pm 1.60\%$	$1.019 \pm 0.10\%$	$0.984 \pm 0.06\%$	$0.0486 \pm 1.80\%$ ($0.0232 \pm 3.0\%$)	$2.52 \pm 0.39\%$ ($1 \pm 0.78\%$)
Changes in flux in percent	47.15	−1.90	0.37	95.14 (97.68)	−152.0 (0)

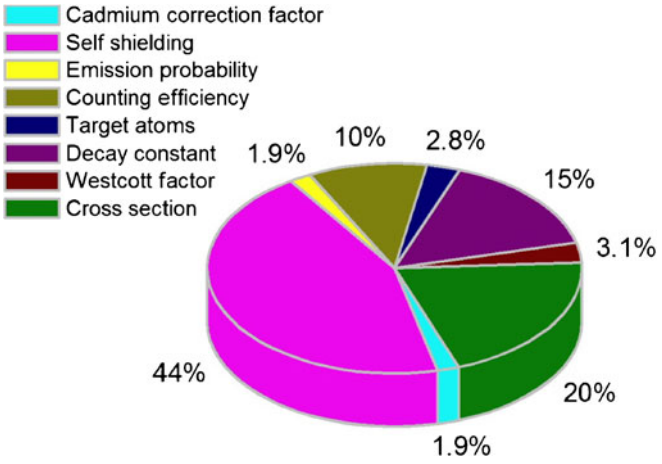

Figure 6. The contribution of various correction factors on the overall uncertainty of thermal neutron flux using NaI(Tl).

factors on overall uncertainty are depicted in figures 6 and 7 for NaI(Tl) and Geiger–Muller counter, respectively. In these figures, very small absolute errors (less than 10^{-5}) were not considered.

3.3 *Thermal neutron flux calculation by simulation*

In order to test the experiment and ensuring the integrity of the results, the set-up was simulated by MCNP4C and thermal neutron flux was determined for these four foils. The simulation outcomes are given in the last column of table 4. It should be mentioned that

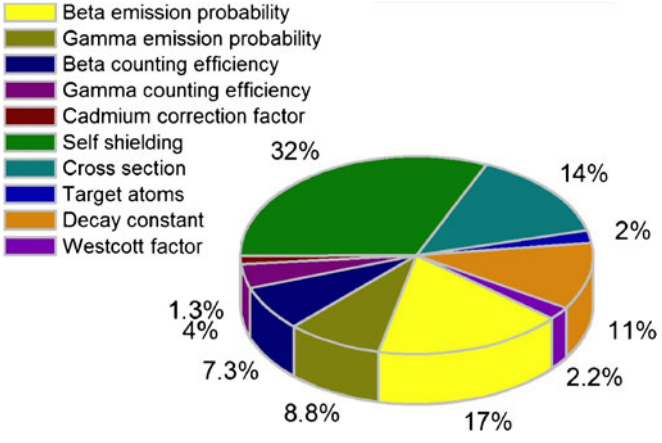

Figure 7. The contribution of various correction factors on the overall uncertainty of thermal neutron flux using Geiger–Muller counter.

Table 6. Relative differences between experiments and simulation.

	Relative difference (%)		
Distance from source (cm)	Geiger and NaI(Tl) (%)	Geiger and simulation (%)	NaI(Tl) and simulation (%)
6	4.7	24	20
8.5	3.7	4.3	0.6
11	4.9	2.7	2.2
13.5	2.7	5.7	3.0

the maximum relative statistical error in the flux calculated using Monte Carlo simulation was almost 0.6%.

The variations between two experimental methods and the simulation are given in table 6. The agreements between experiments and simulation are acceptable except for foil No. 1. This disagreement is partly due to the uncertainty in neutron source position, which has more effect on thermal neutron flux in the foil closest to the source.

According to table 6 the minimum disagreements between the results of Geiger–Muller counter, NaI(Tl) and MCNP4C express the accuracy of experiments. Considering the results, using NaI(Tl) is more suitable to determine thermal neutron flux because of its spectroscopy property which helps in separating the counts due to noises and backgrounds.

4. Conclusion

We measured thermal neutron flux by cadmium difference method using Geiger–Muller counter and NaI(Tl). The results of the two experiments were compared with the MCNP4C simulation and good agreements were observed (except for foil No. 1). Because of its spectroscopy property, using NaI(Tl) is more suitable for determining neutron flux.

References

[1] S Vaughn, *Investigation of a passive, temporal, neutron monitoring system that function within the confines of start* I, M.S. thesis (Air Force Institute of Technology, 2003)
[2] E M Eid Abdel Munem, *Neutron flux measurements with Monte Carlo verification at the thermal column of a Triga mark II reactor: Feasibility study for a BNCT facility*, Ph.D. thesis (Universiti Sains Malaysia, 2008)
[3] F G Knoll, *Radiation detection and measurement*, 3rd edition (John Wiley & Sons Inc, USA, 1999) Vol. 14, p. 505
[4] T M Filho, R B de Lima, H Yoriyaz and A C Hernandes, *Radiat. Prot. Dosim.* **115**, 412 (2005)
[5] E Witkowska, K Szczepaniak and M Biziuk, *Radioanal. Nucl. Chem.* **265**, 141 (2005)
[6] H Yücel and M Karadag, *Ann. Nucl. Energy* **31**, 681 (2004)

[7] M Těšínský, *Measurement and Monte Carlo simulation of the neutron spectra of the sub-critical reactor experiment "Yalina Booster"*, M.Sc. thesis (Czech Technical University, 2006)
[8] T V Blosser and J E Thomas, *Neutron flux and neutron and gamma ray spectra measurements at the HFIR*, Oak Ridge Report for US Atomic Energy Commission, ORNL-TM-2221 (1968)
[9] R M A Maayouf, I I Bashter, W M EL-Maamly and M I Khalil, Neutron flux measurement at the CFDF using different detectors, *IX Radiation Physics & Protection Conference* (2008) p. 67
[10] H Miri Hakimabad and L Rafat Motavalli, *Radiat. Res.* **51**, 123 (2010)
[11] W J Price, *Nuclear radiation detection* (McGraw-Hill, USA, 1964) Vol. 10, p. 341
[12] A Trkov, G Zerovnik, L Snoj and M Ravnik, *Nucl. Instrum. Methods A* **610**, 553 (2009)
[13] C Chilian, J St-Pierre and G Kennedy, *Radioanal. Nucl. Chem.* **278**, 745 (2008)
[14] K Pytel, K Jozefowicze, B Pytel and A Koziel, *Radiat. Prot. Dosim.* **110**, 823 (2004)
[15] A Okazaki and R T Jones, *Radiat. Eff.* **93**, 205 (1986)
[16] T Elnimr, *Appl. Phys.* **23**, 1278 (1990)
[17] http://www.fusor.net/board/view.php?bn=fusor_neutrons&key=1207677526
[18] J Yoon, S Lee, T Ro, S Yamamoto and K Kobayashi, *J. Korean Phys. Soc.* **44**, 809 (2004)
[19] H D Choi, R B Firestone, R M Lindstrom, G L Molnár, S F Mughabghab, R Paviotti-Corcuera, Z Révay, A Trkov, V Zerkin and Z Chunmei, Database of prompt γ rays from slow neutron capture for elemental analysis, IAEA Library Cataloguing in Publication Data (2007)
[20] http://www.orau.org/ptp/PTP%20Library/library/DOE/bnl/nuclidedata/MIRIn116.htm